Oceanic enrichment of ammonium and its impacts on phytoplankton community composition under a high-emissions scenario

Pearse J. Buchanan[1,2,3], Juan J. Pierella Karlusich[4,5], Robyn E. Tuerena[6], Roxana Shafiee[7], E. Malcolm S. Woodward[8], Chris Bowler[9,10], and Alessandro Tagliabue[2]

5 [1]CSIRO Environment, Hobart, 7004, Australia.
   [2]Department of Earth, Ocean and Ecological Sciences, University of Liverpool; Liverpool, L69 3GP, UK.
   [3]Department of Global Ecology, Carnegie Institution for Science; Stanford, CA, 94305, USA.
   [4]FAS Division of Science, Harvard University, Cambridge, MA, 02138, USA.
   [5]Department of Biology, Massachusetts Institute of Technology, Cambridge, MA, 02139, USA.
10 [6]Scottish Association for Marine Science; Dunstaffnage, Oban, PA37 1QA, UK.
   [7]Center for the Environment, Harvard University, Cambridge, MA, 02138.
   [8]Plymouth Marine Laboratory; Plymouth, PL1 3DH, UK.
   [9]Institut de Biologie de l'École Normale Supérieure, Département de Biologie, École Normale Supérieure, CNRS, INSERM, Université de Recherche Paris Sciences et Lettres, Paris, France.
15 [10]CNRS Research Federation for the study of Global Ocean Systems Ecology and Evolution, FR2022/Tara Oceans GEOSEE, Paris, France.

Correspondence to: Pearse J. Buchanan (pearse.buchanan@csiro.au)

Abstract. Ammonium (NH_4^+) is an important component of the ocean's dissolved inorganic nitrogen (DIN) pool, especially in stratified marine environments where intense recycling of organic matter elevates its supply over other forms. Using a global

20 ocean biogeochemical model with good fidelity to the sparse NH_4^+ data that is available, we project increases in the NH_4^+:DIN ratio in over 98% of the ocean by the end of the 21st century under a high-emission scenario. This relative enrichment of NH_4^+ is driven largely by circulation changes, and secondarily by warming-induced increases in microbial metabolism, as well as reduced nitrification rates due to pH decreases. Supplementing our model projections with geochemical measurements and phytoplankton abundance data from *Tara* Oceans, we demonstrate that shifts in the form of DIN to NH_4^+ may impact

25 phytoplankton communities by disadvantaging nitrate-dependent taxa like diatoms while promoting taxa better adapted to NH_4^+. This could have cascading effects on marine food webs, carbon cycling, and fisheries productivity. Overall, the form of bioavailable nitrogen emerges as an potentially underappreciated driver of ecosystem structure and function in the changing ocean.

1 Introduction

30 The chemical species of dissolved inorganic nitrogen (DIN) are fundamental in for the growth of marine primary producers that underpin oceanic food webs, fisheries production and the carbon cycle. Bioavailable DIN is composed of different forms, principally nitrate (NO_3^-), nitrite (NO_2^-) and ammonium (NH_4^+). Typically, NO_3^- is regarded as the main form. This is not without reason, since NO_3^- represents most of the total DIN stock and is prevalent in highly productive regions where it tends

35   to fuel the majority of primary production (Dugdale, 1967). However, NH_4^+ and NO_2^- are recognized as critical fuels for marine primary production in stratified environments, where intense recycling of organic matter can elevate their use by phytoplankton (Clark et al., 2008; Dugdale and Goering, 1967; Fawcett et al., 2011; Rodgers et al., 2024; Yool et al., 2007) and fuel rapid rates of primary production via rapid recycling even if the standing stock of DIN is low (Bender and Jönsson, 2016; Matsumoto et al., 2016; Rii et al., 2016; Yang et al., 2019).

40   The relative speciation of DIN plays a crucial role in shaping marine phytoplankton community composition. Marine diatoms, for instance, show a competitive edge over other types of phytoplankton for growth on NO_3^- as a source of bioavailable nitrogen (Berg et al., 2003; Fawcett et al., 2011; Glibert et al., 2016a; Klawonn et al., 2019; Litchman, 2007; Van Oostende et al., 2017; Selph et al., 2021; Tungaraza et al., 2003; Wan et al., 2018). One theory posits that their ecological success in turbulent, high NO_3^- environments (Margalef, 1978) may be due to a capacity to store NO_3^- in their vacuoles and then rapidly reduce it when

45   they experience sudden increases in light, which would work to use up any excess reductant that would otherwise retard growth (Glibert et al., 2016a; Lomas and Glibert, 1999; Parker and Armbrust, 2005). Meanwhile, other phytoplankton types such as cyanobacteria, more adapted to stable conditions, are considered better competitors for the reduced forms of nitrogen, including NH_4^+ (Fawcett et al., 2011; Glibert et al., 2016a; Litchman et al., 2007) (Fig. 1). There is intense competition for NH_4^+ since nitrogen in this form can be most efficiently converted into glutamate and other basic building blocks for biomass synthesis,

50   while NO_2^- and NO_3^- must be reduced first within the cell (Dortch, 1990). Thus, phytoplankton types with superior affinities for NH_4^+, like cyanobacteria, tend to displace other taxa under nitrogen limiting conditions (Litchman et al., 2007). These competitive outcomes are also well documented in freshwater and brakish systems (Andersen et al., 2020; Carter et al., 2005; Donald et al., 2013; Örnólfsdóttir et al., 2004; Trommer et al., 2020) and appear somewhat universal in aquatic environments.

55   As anthropogenic pressures increase, several factors may tip the balance towards NH_4^+ and other reduced forms of DIN (Fig. 1). Physical changes, including a changing oceanic circulation (Sallée et al., 2021), are expected to limit inputs of NO_3^- from deeper waters to further intensify nitrogen limitation of phytoplankton communities (Bopp et al., 2005; Buchanan et al., 2021). Climate warming is expected to accelerate the metabolism of phytoplankton (Anderson et al., 2021; Eppley, 1972) and thereby increase nitrogen demand and recycling rates (Cherabier and Ferrière, 2022) to potentially elevate reduced forms of nutrients

60   in the lower latitudes (Rodgers et al., 2024). Meanwhile, ocean acidification may decelerate rates of microbial ammonia oxidation, the first step of nitrification (Beman et al., 2011). While it is unlikely that ammonia oxidation would be slowed to the point where substantial quantities of NH_4^+ do not undergo oxidation, a slight deceleration in the upper ocean may elevate the supply ratio of NH_4^+ to NO_3^-. All of these changes are expected to increase the relative availability and/or supply of NH_4^+ compared to the more oxidized forms of NO_2^- and NO_3^-. Due to the intense competition for NH_4^+ and resulting shifts towards

65   smaller phytoplankton taxa that are more rapidly recycled in the upper water column, the relative enrichment in NH_4^+ may become a self-sustaining regime. However, the magnitude of NH_4^+ enrichment and its dominant drivers remain unquantified. Moreover, even though there are numerous localized studies that showcase how phytoplankton taxa shift in response to changes

in the composition of DIN, we lack a general understanding of the degree to which phytoplankton communities are affected by the relative enrichment of NH_4^+ at the global scale. This represents an important knowledge gap as to how climate change

70   will affect the upper ocean nitrogen cycle and phytoplankton community composition, with possible implications for carbon export and fisheries productivity.

In this work, we use a global ocean-biogeochemical model equipped with an advanced nitrogen cycle to quantify the relative enrichment of NH_4^+ enrichment within a future ocean. Hereafter, we use the NH_4^+ to dissolved inorganic nitrogen ratio

75   (NH_4^+:DIN), where DIN = NH_4^+ + NO_2^- + NO_3^-, as a measure of this relative availability in the form of nitrogen. When we refer to the relative enrichment of NH_4^+, we specifically mean an increase in the amount of DIN that is NH_4^+, with an enrichment consistent with a higher proportion of primary production supported through regeneration (i.e., NH_4^+-fueled). We comment on the potential ecological importance of this enrichment by using compilations of phytoplankton relative abundance data collected during the *Tara* Oceans expeditions and idealized experiments that isolate the effect of competition for NH_4^+

80   from NO_3^-.
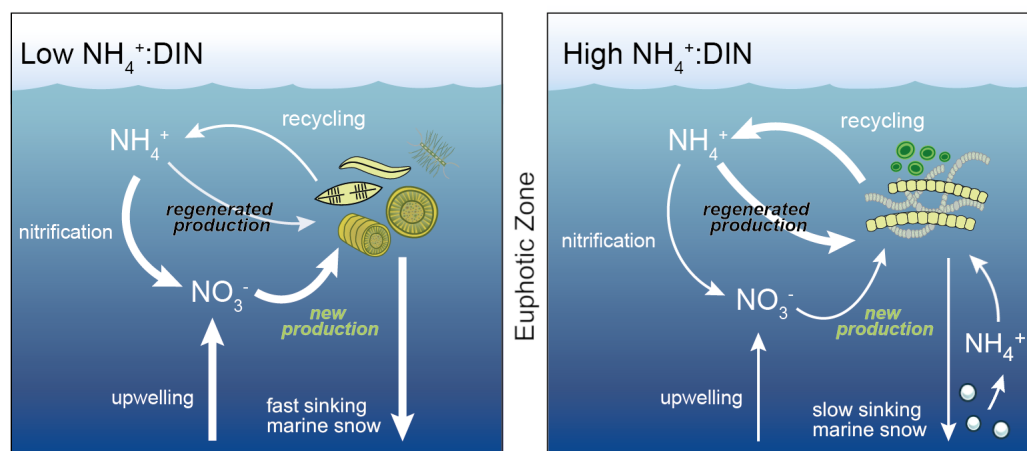
Figure 1. Regimes of low NH_4^+:DIN and higher NH_4^+:DIN regimes in the upper ocean. In a low NH_4^+:DIN regime, there is more vertical delivery of NO_3^- to the euphotic zone through physical mixing, which is taken up by larger phytoplankton (termed new production), including diatoms, to produce larger, denser aggregates of sinking organic matter (marine snow) that undergo recycling deeper in the water column.
85   In the high NH_4^+:DIN regime, less NO_3^- is mixed into the euphotic zone and NH_4^+ supports a greater proportion of primary production (termed regenerated production). Those phytoplankton that are competitive for NH_4^+ tend to be smaller, and form less dense aggregates that sink more slowly. Consequently, more organic matter is recycled within the euphotic zone and there is more regenerated production.

2 Materials and Methods

90 **2.1 The biogeochemical model**

The biogeochemical model is the Pelagic Interactions Scheme for Carbon and Ecosystem Studies version 2 (PISCES-v2) (Aumont et al., 2015). This model is embedded within version 4.0 of the Nucleus for European Modelling of the Ocean (NEMO-v4.0). We chose a 2° nominal horizontal resolution with 31 vertical levels with thicknesses ranging from 10 meters in the upper 100 meters to 500 meters below 2000 meters. Due to the curvilinear grid, horizontal resolution increases to 0.5° 95 at the equator and to near 1° poleward of 50°N and 50°S.

We updated the standard PISCES-v2 for the purposes of this study (see Supplementary Text S1 for a detailed description of the additions). This model explicitly resolves the pools of NH_4^+, NO_2^-, NO_3^-, two kinds of phytoplankton biomass (nanophytoplankton and diatoms), two kinds of zooplankton biomass (micro- and meso-zooplankton), small and large pools 100 of particulate organic matter, and dissolved organic matter. Nitrogen is added to the ocean via biological nitrogen fixation, riverine fluxes, and atmospheric deposition. Nitrogen is removed from the ocean via denitrification, anaerobic ammonium oxidation (anammox) and burial. The internal cycling of nitrogen involves assimilation by phytoplankton in particulate organic matter, grazing and excretion by zooplankton, solubilization of particulates to dissolved organics, ammonification of dissolved organic matter to NH_4^+, followed by nitrification of NH_4^+ and NO_2^- via ammonia oxidation and nitrite oxidation. Nitrification 105 in this version of PISCES-v2 is now split into its two component steps (ammonia and nitrite oxidation) for the purposes of this study, and both steps are made to be a function of substrate availability, light, and in the case of ammonia oxidation, pH (Supplementary Text S1). The model shows good fidelity to the available observations of NH_4^+ concentrations, NH_4^+:DIN ratios, and rates of NH_4^+ cycling that we compiled for this study (Supplementary Text S2; Fig. S1-S3).

110 **2.2 Model experiments**

To quantify the impact of anthropogenic activities on NH_4^+:DIN ratios, we performed transient simulations by forcing the biogeochemical model with monthly physical outputs produced by the Institut Pierre-Simon Laplace Climate Model 5A (Dufresne et al., 2013). Simulations included a preindustrial control where land-use, greenhouse gases and ozone remained at preindustrial conditions, and a climate change run where these factors changed according to historical observations from 1850 115 to 2005 and according to the high emissions Representative Concentration Pathway 8.5 from 2006 to 2100 (RCP8.5) (Riahi et al., 2011). We chose a high emissions scenario to emphasize the clearest degree of anthropogenic changes, and thus maximize anthropogenic effects. However, we acknowledge that the RCP8.5 is considered an extreme scenario under present development pathways (Riahi et al., 2017).

120   In addition, we performed parallel experiments that isolated the individual effects of our three anthropogenic stressors: a changing circulation ("Phys"), warming on biological metabolism ("Warm"), and acidification effects on ammonia oxidation ("OA"). The experiment with all anthropogenic effects was termed "All". These experiments involved altering the factor of interest in line with the historical and RCP8.5 scenario while holding the other factors at their preindustrial state.

125   The effect of climate change at the end of the 21st century (mean conditions 2081-2100) was quantified by comparing with the preindustrial control simulation. This preindustrial control simulation was run parallel to the climate change simulations (i.e., 1850-2100), but without anthropogenic forcings. This allowed a direct comparison to be made between experiments at the end of the 21st century and eliminated the effect of model drift. We calculated changes at each grid cell by averaging over the euphotic zone, which was defined as those depths where total phytoplankton biomass was greater than 0.1 mmol C m^{-3}. In

130 addition, we compared the preindustrial simulation with observations to explore broad patterns in NH_4^+ and NH_4^+:DIN ratios, averaged over the euphotic zone.

   Finally, we repeated the set of experiments described above (All, Phys, Warm and OA) but with an alternative parameterization where diatoms were made to have the same growth limitation on NH_4^+ as other phytoplankton. This experiment was called

135 "model$_{compete}$", while the model with the default parameterization for nitrogen limitation was termed "model$_{control}$".

2.3 Nutrient and rate data

   Measured NH_4^+ concentrations (N=692) were used for model-data assessment (Fig. S2-S3). Nutrients were collated from published work (Buchwald et al., 2015; Mdutyana et al., 2020; Newell et al., 2013; Raes et al., 2020; Santoro et al., 2013,

140 2021; Shiozaki et al., 2016; Tolar et al., 2016; Wan et al., 2018, 2021), and oceanographic cruises AR16 (https://www.bco-dmo.org/deployment/747056), JC156, and JC150. Coincident NO_2^- and NO_3^- were used to compute NH_4^+:DIN ratios. If coincident measurements of NO_2^- were not available, then NH_4^+:DIN ratios were calculated with only NO_3^-. If NO_3^- measurements were not made alongside NH_4^+, then NO_3^- concentrations were extracted from the World Ocean Atlas 2018 (Garcia et al., 2019) monthly climatology at the closest grid cell. These data are available in Data Set S1.

145

   Measured ammonia oxidation rates (N=696) were also used for model-data assessment and showed broad agreement with the model (Fig. S3). Data were collated from published work (Clark et al., 2021; Dore and Karl, 1996; Mdutyana et al., 2020; Newell et al., 2013; Raes et al., 2020; Raimbault et al., 1999; Santoro et al., 2013, 2021; Shiozaki et al., 2016; Tolar et al., 2016; Wan et al., 2018, 2021) and are available in Data Set S2.

150

   Measurements of NH_4^+ and NO_3^- concentrations alongside NH_4^+- and NO_3^--fueled primary production (μmol m^{-3} day^{-1}) were used to determine the relationship between NH_4^+:DIN ratios and the proportion of net primary production that is fueled by

NH$_4^+$. While coincident measurements of these properties are not common, we compiled data from nine studies (Fernández et al., 2009; Joubert et al., 2011; Mdutyana et al., 2020; Metzler et al., 1997; Philibert, 2015; Rees et al., 2006; Thomalla et al.,

155   2011; Wan et al., 2018; Yingling et al., 2021) providing 190 data points that together encompassed oligotrophic to eutrophic conditions from the tropics to the Southern Ocean. Measurements from the Gulf of Mexico (Yingling et al., 2021) were unique in that nutrient concentrations and uptake rates were not measured at precisely the same depths or stations. Coincident values were determined by calculating trends in depth via linear interpolation (Fig. S4). These data are available in Data Set S3.

160   Ammonia oxidation rates data from experiments involving pH changes were acquired directly from the papers presenting the results (Beman et al., 2011; Huesemann et al., 2002; Kitidis et al., 2011) by extraction from the text (where values were given) and from figures using the WebPlotDigitizer tool (https://automeris.io/WebPlotDigitizer/). Changes in ammonia oxidation rates were normalized to a pH of 8 (Fig. S5). These data are available in Data Set S4.

165   **2.4 Phytoplankton relative abundance data**

Tara Oceans expeditions between 2009 and 2013 performed a worldwide sampling of plankton in the upper layers of the ocean (Pierella Karlusich et al., 2020). We mined the 18S rRNA gene (V9 region) metabarcoding data set (Ibarbalz et al., 2019; de Vargas et al., 2015) by retrieving the operational taxonomic units (OTUs) assigned to eukaryotic phytoplankton from samples obtained from 144 stations (https://zenodo.org/record/3768510#.Xraby6gzY2w). Barcodes with greater than 85 % identity to

170   phytoplankton sequences in reference databases were selected. The total diatom barcode reads in each sample was normalized to the barcode read abundance of eukaryotic phytoplankton. We exclusively used the data sets corresponding to surface samples (5-9 m depth).

In addition, we analyzed the metagenomic read abundances for the single-copy photosynthetic gene *psbO*, an approach that

175   covers both cyanobacteria and eukaryotic phytoplankton and provides a more robust picture of phytoplankton cell abundances than rRNA gene methods (Pierella Karlusich et al., 2023). We retrieved the abundance tables from samples obtained from 145 stations (https://www.ebi.ac.uk/biostudies/studies/S-BSST761).

2.5 Statistical analyses

180   We explored the environmental drivers of change in phytoplankton relative abundance data (provided by *Tara* Oceans) with generalized additive models (GAMs) using the *mgcv* package in R (Wood, 2006) according to the equation:

$$Y = +s_1(x_1) + s_2(x_2) + \cdots + s_n(x_n) + \varepsilon, \tag{1}$$

Where Y is the predicted value of the response variable, α is the intercept, $s_n(x_n)$ is the nth thin-plate spline of the nth independent variable, and ε is the population error around the prediction. Independent variables were mixed-layer depth (m), phosphate (μM), silicate (μM), dissolved iron (μM), and the NH_4^+:DIN ratio. Mixed layer depth, phosphate and silicate was measured *in situ* at the sample locations of Tara Oceans, while dissolved iron and NH_4^+:DIN ratios were provided by the model. In addition, phosphate and silicate concentrations were available as interpolated products from the World Ocean Atlas (Garcia et al., 2019). An alternative estimate of NH_4^+:DIN ratios was provided by the Darwin model (Follows et al., 2007). Predictor variables from models and World Ocean Atlas were extracted at the locations and months of sampling. Mixed-layer depth, nutrients (phosphate, silicate and NH_4^+:DIN) and the relative abundance of phytoplankton taxa were $\log_{10}$-transformed prior to model building to ensure homogeneity of variance.

Before model testing, we calculated the variance inflation factors (VIFs) of independent variables to avoid multi-collinearity. All covariate VIFs were < 3. GAMs were computed using a low spline complexity (k = 3) that prevented overfitting. We fit GAMs using all predictors (full model), then assessed the deviance explained by each predictor by fitting subsequent GAMS with each predictor in isolation, and by removing the predictor in question from the full model. The significance of a predictor was assessed by applying a smoothing penalty to only that predictor in the full model. Diagnostic plots were assessed visually, and predictive capacity was assessed via the percent of deviance explained by the model.

A two-sided Mann-Whitney U test was used to test for differences between the two distributions of diatom relative abundance separated by NH_4^+:DIN ratios < 4% and > 4%. The 4% threshold was used because it split the dataset in half and aligned with the point at which primary production transitioned from mostly new (NO_3^--fueled) to regenerated (NH_4^+-fueled). This non-parametric test (performed with the *scipy* package in python) returned highly significant two-sided p-values (p < 0.0001) as indicated by ***.

3 Results and Discussion

3.1 Future enrichment of NH_4^+ in the ocean and its drivers

Given the potential importance of NH_4^+ enrichment for influencing the balance between regenerated and new primary production and phytoplankton community composition, we estimated the potential impact of anthropogenic climate change on NH_4^+:DIN across the global ocean. Using a high emissions climate change scenario from 1851 to 2100 (Representative Concentration Pathway 8.5 (Riahi et al., 2011)), we simulated physical changes (circulation change + sea-ice loss), the stimulation of metabolism by warming, and a data-informed slowdown of ammonia oxidation by ocean acidification (Fig. S5) in our ocean-biogeochemical model. We note that the model effectively reproduced the broad-scale patterns in observed NH_4^+

215 concentrations, NH_4^+:DIN ratios and patterns in NH_4^+ cycling between oligotrophic and eutrophic regimes in the contempory ocean (Supplementary Text S2; Fig. S1-S3) and was therefore well placed to investigate changes in DIN speciation.

By the end of the 21st century (2081-2100), NH_4^+:DIN is projected to increase in over 98% of the upper ocean euphotic layer (Fig. 2a). On average, the fraction of DIN present as NH_4^+ increased by 6 ± 6 %, with enrichment exceeding 20% in regions with pronounced DIN gradients, such as oceanographic fronts. The enrichment of NH_4^+ caused an expansion of regenerated

220 production across the ocean, such that NH_4^+ overtook NO_3^- as the main nitrogen substrate for phytoplankton growth in an additional 13% of the ocean. The greatest changes occurred within the 21st century (Fig. 2b), indicating a direct relationship between the severity of climate change and the magnitude of NH_4^+ enrichment.

Physical changes, a warming-induced stimulation of microbial metabolism, as well as ocean acidification all played a role in

225 increasing NH_4^+:DIN. Among these factors, physical changes had the largest contribution, accounting for 55% of future trends (Fig. 2b). Physical changes decreased DIN to cause increases in NH_4^+:DIN in many regions (Fig 2c; Fig. S6) and occurred either through reduced physical supply (e.g., North Atlantic (Whitt and Jansen, 2020)) or increased demand and export of organic nitrogen in regions experiencing an increase in primary production due to losses in sea ice and increases in light (e.g., Arctic (Comeau et al., 2011)).

230

Ocean acidification, responsible for 25% of the NH_4^+:DIN increases, increased NH_4^+:DIN ubiquitously, but had the greatest effect in oligotrophic settings where DIN concentrations were lower, and minimal effects in eutrophic regions (Fig 2c; Fig. S6). We do note, however, that there is much uncertainty in the relationship between pH and ammonia oxidation rates (Bayer et al., 2016; Kitidis et al., 2011). To accommodate some of this uncertainty, we performed an idealized experiment with a

235 much weaker relationship between pH and ammonia oxidation. This reduced the influence of acidification by 10% or more and increased the contribution of the other stressors (Fig. S7). The effect of pH decline was, however, only influential to NH_4^+:DIN ratios in the subtropical gyres where NH_4^+:DIN ratios were already high. Thus, whether pH declines have a strong or weak effect on ammonia oxidation did little to change NH_4^+:DIN ratios in eutrophic regions, where coincidentally, shifts from low to higher NH_4^+:DIN would have the greatest ecological impact.

240

Warming stimulated the nutrient demand of phytoplankton, which reduced DIN, a mechanism consistent with the effects of temperature on marine microbial recycling (Cherabier and Ferrière, 2022). While its global contribution was small at 13% (Fig. 2b), the stimulation of microbial metabolism had important effects at the boundaries of NO_3^--rich regions by contracting their areal extent, turning previously NO_3^--rich waters to NO_3^--poor waters (Fig. 2c; Fig. S6). Altogether, the individual

245 contributions of physical change, acidification and stimulated metabolism diagnosed via our sensitivity experiments explained 93% of the full change in NH_4^+:DIN, indicating small interactive effects and therefore that a linear combination of the three drivers accounted for near the full response.
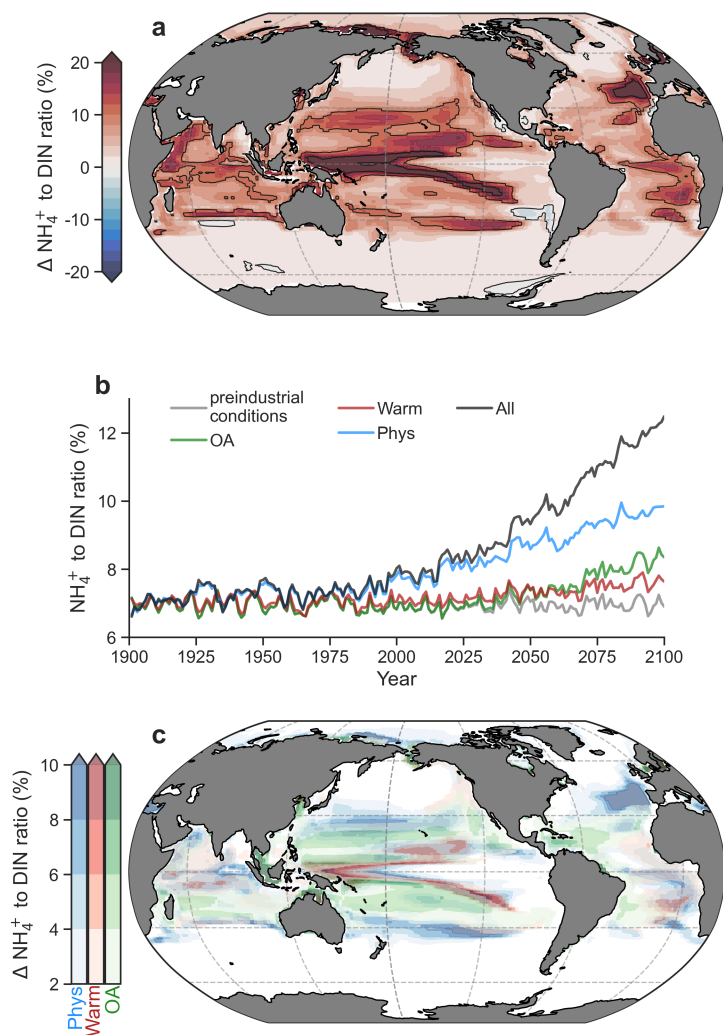
Figure 2. Anthropogenic impacts on the NH_4^+ to DIN ratio in a high-emissions scenario. (a), The difference in the NH_4^+ to DIN ratio averaged over the euphotic zone at the end of the 21st century (2081-2100) with all anthropogenic impacts. (b), Global mean trends in euphotic zone NH_4^+ to DIN ratio in the different experiments: preindustrial control (grey), ocean acidification (OA; green), warming on metabolic rates (Warm; red), physical changes (Phys; blue) and all effects (All; black) according to the RCP8.5 climate change scenario. (c), Increases in the NH_4^+ to DIN ratio due to physical changes (blue), effect of warming on metabolic rates (red) and ocean acidification on ammonia oxidation (green) from a multiple stressor perspective.

3.2 Simulated impacts on phytoplankton community composition

The biogeochemical model accounts for two phytoplankton functional types: a nanophytoplankton and a diatom type (Aumont et al., 2015). Our climate change simulations projected a future decline in the relative abundance of diatoms, particularly in
260   the subantarctic, tropical, North Atlantic, North Pacific and Arctic Oceans where declines sometimes exceeded 20% (Fig. 3a; Fig. S8). Our sensitivity experiments enabled an attribution of the major drivers, at least in a coarse grained sense. The loss of diatom representation within marine communities in our model was driven by a combination of stimulated microbial metabolism (60%) and physical changes (40%), while ocean acidification had negligible effects (Figure 3b; Fig. S8). Such declines have been predicted previously and are widely accepted to be due to a decline in bulk nutrient availability in the upper
265   ocean (Bopp et al., 2005), although the large effect of stimulated metabolism here suggests that top-down grazing pressure, which is accelerated by warming, also very likely plays a role (Chen et al., 2012; Rohr et al., 2023). That said, stimulating metabolism also increases phytoplankton nutrient demand, which eventually leads to greater DIN limitation (Cherabier and Ferrière, 2022). We indeed appreciate that the reduction of diatoms from phytoplankton communities as simulated by models is due to nutrient losses, in particular declines in NO_3^- (Kwiatkowski et al., 2020), and our simulations here, in some ways, are
270   no different.

However, models that explicitly represent NH_4^+ are able to provide a more nuanced view of why a decline in NO_3^- might cause a decline in diatom relative abundance, or shifts in any phytoplankton taxa for that matter. We cast this view specifically in terms of an increase in competition for NH_4^+, and base this on two lines of evidence. First, a decline in the standing stock of
275   DIN does not mean a decrease in its supply. In fact, rapid rates of primary production are measured in nutrient poor waters, which implies rapid recycling and thus a rapid resupply of DIN in the form of NH_4^+ (Bender and Jönsson, 2016; Matsumoto et al., 2016; Rii et al., 2016; Yang et al., 2019). This is akin to the bathtub analogy, wherein the same inflow (productivity) can result in different volumes (i.e, nutrient concentration) by varying the outflow (i.e., recycling). Second, we take at face value the lower measured NH_4^+ affinities of diatoms compared with other phytoplankton (Litchman, 2007; Litchman et al.,
280   2007), and we account for this competitive disadvantage explicitly in our ocean biogeochemical model (Fig. 3c). The combination of intense competition for rapidly supplied NH_4^+ and the poor competitive ability of diatoms for NH_4^+ suggests that when NO_3^- concentrations decline, competition for NH_4^+ increases, and declines in diatom relative abundance follow.

We recognize that other influential bottom-up and top-down stressors, such as growth limitation by other nutrients (Taucher
285   et al., 2022), shifts in the light environment, and/or grazing pressure (Brun et al., 2015; Margalef, 1978; Taucher et al., 2022) are also influential to structuring phytoplankton communities. The fact that a warming-induced stimulation of metabolism was linked to 60% of the diatom declines, for instance, could be due to a wide array of factors, not just the resulting increase in NH_4^+:DIN. Furthermore, we acknowledge that if a negative correlation between NH_4^+:DIN and diatom relative abundance exists, in our model or any observations, that thid negative correlation may be confounded by covariates. If other factors are

290   covarying with the NH_4^+:DIN ratio but are more influential to diatom relative abundance, this may lead to the erroneous attribution of a causative relationship between diatom relative abundance and NH_4^+:DIN ratios (i.e., a false positive). Most importantly for our study, there is clearly a strong correlation between NO_3^- concentrations and NH_4^+:DIN ratios, as increasing NO_3^- decreases NH_4^+:DIN ratios and *vice versa*. It is therefore possible that reductions in NO_3^- and resulting competition for NO_3^- was a major contributor to the losses of diatoms from the phytoplankton community in our simulations (Fig. 3a).

295

We therefore sought to isolate the impact of competition for NH_4^+ specifically, and thus target the causative relationship between NH_4^+:DIN and diatom relative abundance. To do so, we performed idealized experiments that equalized diatom growth limitation on NH_4^+ with that of other phytoplankton, so that there was zero competitive advantage or disadvantage for NH_4^+ between these groups. This simulation was called "model$_{compete}$", and was equivalent to making the dashed black and

300   green lines in Figure 3c exactly the same under all conditions (see upward arrow in Fig. 3c). All other traits remained unchanged. Importantly, this included the different affinities of diatoms and other phytoplankton for NO_3^-, for which diatoms have a competitive advantage at high NO_3^- but a competitive disadvantage at low NO_3^-. In other words, when DIN was low, diatoms were equally competitive for NH_4^+, but still suffered their unique limitations associated with light, silicate, phosphate, NO_3^- and iron availability, as well as grazing pressure.

305

Surprisingly, making diatoms equally competitive for NH_4^+ mitigated the losses of diatom representation within future phytoplankton communities by 70% (Fig. 3d). Losses in NO_3^- still occurred in these experiments, and these losses in NO_3^- caused declines in phytoplankton productivity and in particular the productivity of diatoms, whom are disadvantaged compared to the nanoplankton functional type under low NO_3^-. While phytoplankton biomass, including diatoms, largely declined

310   everywhere outside of the polar regions (Fig. S8), the losses in diatom relative abundance were only 0.9% by 2081-2100 (Fig. 3e). Physical changes no longer exerted a global negative effect on their total nor relative abundance (blue line in Fig. 3e), while the negative effect of elevated microbial metabolism on relative abundance was ameliorated by 25% (Fig. 3e; Fig. S8-S9). Diatoms even showed increased total and/or relative abundance in regions where previously there were losses, including the Arctic, the tropical Pacific, the Arabian Sea, the North Atlantic, and the southern subtropics (Fig. 3d; Fig. S9). Outside of

315   the Southern Ocean and the eastern boundary upwelling systems, physical changes that tended to reduce DIN concentrations now favored diatoms, while elevated metabolism now had positive, rather than negative, effects in the tropical Pacific.

These experiments provide some potential insights into the factors controlling diatom niches in the global pelagic ocean. Regions where our control experiment, "model$_{control}$", and model$_{compete}$ show similar changes are regions where other factors

320   besides NH_4^+ supply determine diatom competitiveness. A good example is the Southern Ocean, where iron, light and silicic acid are the major controls on diatom productivity and phytoplankton community composition (Boyd et al., 1999, 2000; Krumhardt et al., 2022; Llort et al., 2019). Accordingly, there is close correspondence in the model, evident by the in the

matching outcomes of model$_{control}$ and model$_{compete}$. However, where model$_{control}$ and model$_{compete}$ predicted contrasting outcomes, the form of nitrogen, specifically NH$_4^+$:DIN and thus the intense competition for NH$_4^+$, exerted a dominant control.

325
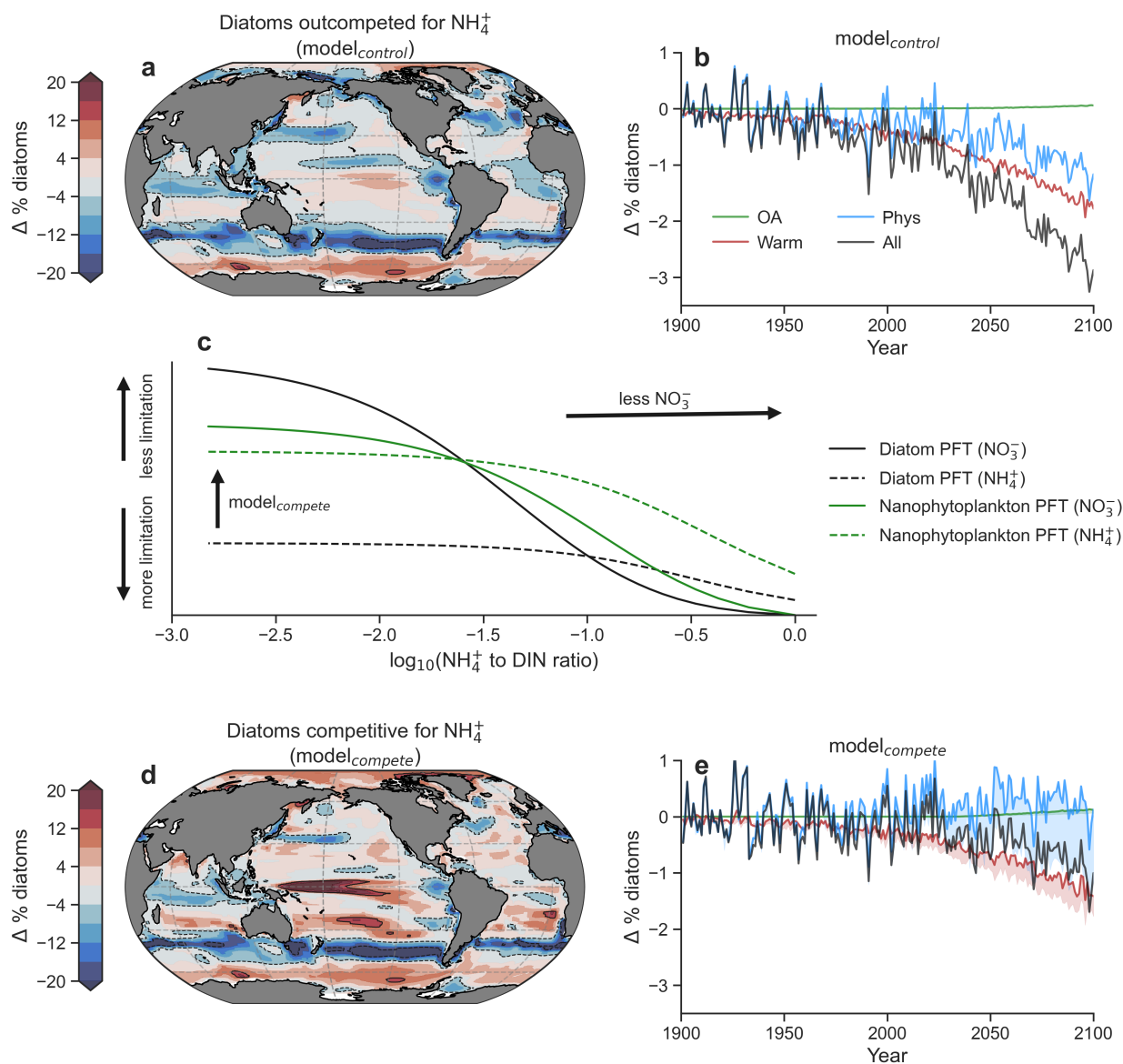
Figure 3. Impact of NH$_4^+$ enrichment within DIN on diatom relative abundance. (a), Mean change (Δ) in the relative abundance of diatoms (%) by the end of the 21st century (2081-2100) as predicted by the control run of the ocean-biogeochemical model (model$_{control}$) under the RCP8.5 scenario and averaged over the euphotic zone. (b), Global mean change in diatom relative abundance due to physical (circulation + light) changes (blue), warming effects on metabolic rates (red), ocean acidification effect on ammonia oxidation (green) and all stressors (black) for model$_{control}$. (c), Limitation of the diatom (black) and nanophytoplankton (green) phytoplankton functional types (PFT) in the ocean-biogeochemical model by NO$_3^-$ (solid lines) and NH$_4^+$ (dashed lines) as a function of the NH$_4^+$:DIN ratio on a log$_{10}$ scale. Note that

the nanophytoplankton PFT is always more competitive for NH_4^+ and is more competitive for NO_3^- when NO_3^- is low. (d), The same as in (a), but for model$_{compete}$, where the NH_4^+ growth limitation of the diatom PFT was made equal to the nanophytoplankton PFT. (e), The same

335 as in (b), but for model$_{compete}$. The shading shows the change between model$_{control}$ and model$_{compete}$.

3.3 Can we build confidence using observations?

So far, we have projected widespread increases in NH_4^+:DIN in a high-emissions scenario and determined that a large fraction

of the projected declines in diatom relative abundance are due to their competitive exclusion by other phytoplankton in regions

340 where NH_4^+ becomes more important as a nitrogen source. However, what do the observations tell us? Can this negative

relationship between NH_4^+:DIN and diatom relative abundance be observed at a global scale? Evidence for local extirpation

of diatoms by taxa more competitive for NH_4^+ has been reported by many studies (Andersen et al., 2020; Carter et al., 2005;

Donald et al., 2013; Glibert et al., 2016a; Örnólfsdóttir et al., 2004; Trommer et al., 2020), but is the relationship strong enough

to play out across the wide biogeographic regimes in the ocean? Furthermore, is the parameterization of our model showcased

345 in Figure 3c realistic? Does it reproduce observed shifts from new to regenerated production as NH_4^+ increases?

3.3.1 NH_4^+:DIN and regenerated production

We address the latter question first. If the model cannot reproduce observed shifts from NO_3^- to NH_4^+ fuelled primary

production as NH_4^+:DIN changes, then we might be less confident in its projected increases in regenerated production, and by

350 extension less confident in the magnitude of projected declines in diatom relative abundance. We collated parallel observations

of NH_4^+:DIN ratios and rates of new and regenerated production from studies spanning tropical to polar environments

(Fernández et al., 2009; Joubert et al., 2011; Mdutyana et al., 2020; Metzler et al., 1997; Philibert, 2015; Rees et al., 2006;

Thomalla et al., 2011; Wan et al., 2018; Yingling et al., 2021). Such coincident measurements are rare. Nonetheless, this

compilation was able to show the expected positive relationship between the NH_4^+:DIN ratio and the proportion of primary

355 production that is regenerated (Fig. 4). While this relationship is expected, in that high NH_4^+ to DIN ratios should coincide

with high rates of regenerated primary production, the functional form of this relationship is important yet not well known.

The compilation of studies reveals that it is sharp and non-linear, and here we describe it using a quadratic Monod function

with an optimal half-saturation constant of 0.2 ± 0.03 and an exponent of 0.5 ± 0.05 (Pearson's correlation = 0.69; R^2

(coefficient of determination) = 0.47; as compared to a linear relationship with an R^2 (coefficient of determination) = -1.13)).

360 This quadratic function predicts that regenerated production contributes half of total net primary production when the standing

stock of NH_4^+ is only 4 ± 3 % of total DIN. The data at hand therefore suggest that phytoplankton grow principally on NH_4^+

(regenerated production) and only transition to using NO_3^- when NH_4^+ is substantially depleted to concentrations at or below

4% of total DIN.

365   A similarly sharp relationship emerged from our global ocean-biogeochemical model (Aumont et al., 2015) (grey dots in Fig.

4). This builds confidence in our projected increases in regenerated production as a consequence of increasing NH_4^+:DIN

ratios, but why did the model behave similarly to the observed relationship? In the model, all phytoplankton are parameterized

to have higher affinities for NH_4^+, consistent with laboratory studies (Litchman, 2007; Litchman et al., 2007). Their growth is

supported by NH_4^+ only until NO_3^- becomes sufficiently abundant to allow for higher growth rates (Fig. 3c). In the model, this

370   transition from NH_4^+ to NO_3^- fuelled growth occurs at NH_4^+:DIN ratios of roughly 0.1 for the diatom functional type and

roughly 0.025 for the nanophytoplankton function type under typical conditions. Hence, our model represents accelerated

growth on NO_3^- in both phytoplankton function types but only at very low NH_4^+:DIN ratios, and thus reproduces the sharp

functional form that is observed.

375
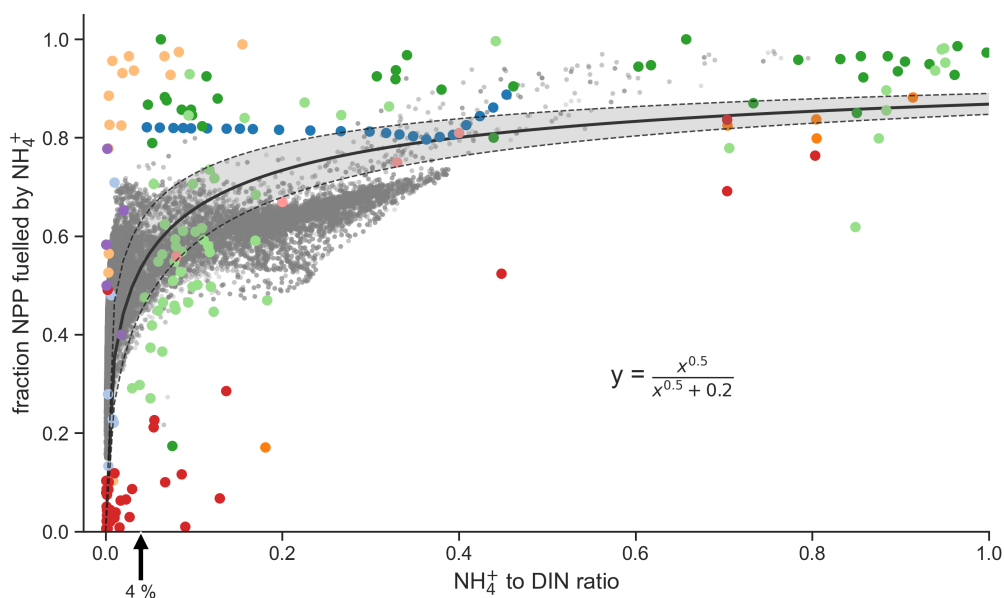
Figure 4. Coincident measurements of the NH_4^+ to DIN ratio and the fraction of net primary production (NPP) fuelled by NH_4^+ from nine studies (coloured dots) and as output by the ocean biogeochemical model (grey dots). Black solid line is the best fit line to the observations and is described by the equation. Shading denotes one standard deviation.

380   **3.3.2 NH_4^+:DIN and phytoplankton community composition**

Next, we search for evidence of a relationship between NH_4^+:DIN ratios and phytoplankton community composition in the

global ocean. While evidence from many localized studies in freshwater, brackish and marine environments suggests that

increasing NH_4^+:DIN ratios should have an effect on phytoplankton community composition, namely a negative effect on

diatom relative abundance and a positive effect on cyanobacterial relative abundance (Berg et al., 2003; Carter et al., 2005;

385 Donald et al., 2013; Fawcett et al., 2011; Klawonn et al., 2019; Van Oostende et al., 2017; Selph et al., 2021; Tungaraza et al., 2003; Wan et al., 2018), evidence for this relationship across the large-scale of the global ocean is lacking.

The *Tara* Oceans global survey offers 144 stations encompassing equatorial to polar marine environments (Ibarbalz et al., 2019). We used two proxies of phytoplankton relative abundance from this dataset: 18S rRNA gene metabarcodes for
390 estimating relative abundance among eukaryotes (de Vargas et al., 2015), and *psbO* gene counts for estimating relative abundance among all phytoplankton (cyanobacteria and eukaryotes) (Pierella Karlusich et al., 2023). These estimates were combined with NH_4^+:DIN as predicted by our global ocean-biogeochemical model at the same location and month of sampling, since real NH_4^+ measurements are scarce. This model effectively reproduced the sparse available datasets of NH_4^+ and NH_4^+:DIN, and is aligned with current understanding of how NH_4^+ cycles in the ocean (Supplementary Text S2; Fig. S1-S3).
395 The model-derived NH_4^+:DIN and other important environmental variables were used to predict relative abundances of major phytoplankton taxa via Generalized Additive Models (GAMs; see Methods).

Our analysis revealed that what has been observed at local scales is apparent in the global *Tara* Oceans dataset. Essentially, elevated NH_4^+:DIN was consistently associated with declines in diatom relative abundance (Fig. 5a). The negative relationship
400 between NH_4^+:DIN and diatom relative abundance was evident and significant in GAMs trained on both abundance proxies (18S rRNA and *psbO* gene counts), as well as when using different combinations of predictor variables: whether model-derived, *in situ* measurements, interpolated products (Garcia et al., 2019), or even when switching out NH_4^+:DIN as predicted by our biogeochemical model with that provided by another (Follows et al., 2007) (Table S1). Importantly, the relationship between NH_4^+:DIN and diatom relative abundance remained consistently negative and significant despite the combination of
405 predictor variables, which builds confidence in the statistical relationship. This was not the case for other predictors (phosphate, silicate, dissolved iron and mixed layer depth), which were prone to insignificance or sign changes depending on the combination of predictors used (Fig. S10-S14). NH_4^+:DIN also offered large explanatory power for diatom abundance compared to the other predictor variables, explaining between 18-30% of the deviance in the data (Table S1).

410 We also saw some strong associations between NH_4^+:DIN and the relative abundance of dinoflagellates, *Prochlorococcus* and chlorophytes (Table S2; Fig. S15-S16). *Prochlorococcus* was positively related to NH_4^+:DIN, as expected, reflecting their superior affinity for NH_4^+ and dominance in oligotrophic gyres (Herrero et al., 2001; Litchman, 2007; Litchman et al., 2007; Matsumoto et al., 2016; Rii et al., 2016). The positive relationship between dinoflagellates and NH_4^+:DIN within eukaryotic phytoplankton, but not in the *psbO* gene counts, likely reflects the inclusion of non-photosynthetic (i.e., heterotrophic)
415 dinoflagellate lineages with the 18S metabarcoding method that are excluded form the *psbO* method (Pierella Karlusich et al., 2023), and the proliferation of these types within systems enriched in reduced nitrogen (Glibert et al., 2016b). Like diatoms, chlorophytes were negatively related to NH_4^+:DIN. Interestingly, this is contrary to the outcomes of the freshwater studies that suggest a seasonal succession of increased chlorophyte concentrations as NH_4^+ concentrations increase following a diatom

bloom on NO_3^- (Andersen et al., 2020), as well as the high affinities that chlorophytes appear to have for NH_4^+ over NO_3^-
420 (Litchman, 2007; Litchman et al., 2007). However, the relative abundance of marine chlorophytes may also be affected by intense competition for NH_4^+ with cyanobacteria, which may have the competitive edge over small eukaryotes and push these taxa to niches with higher nutrient availability (Vannier et al., 2016). For chlorophytes, we therefore see a different relationship at the global scale compared to the local scale.

425
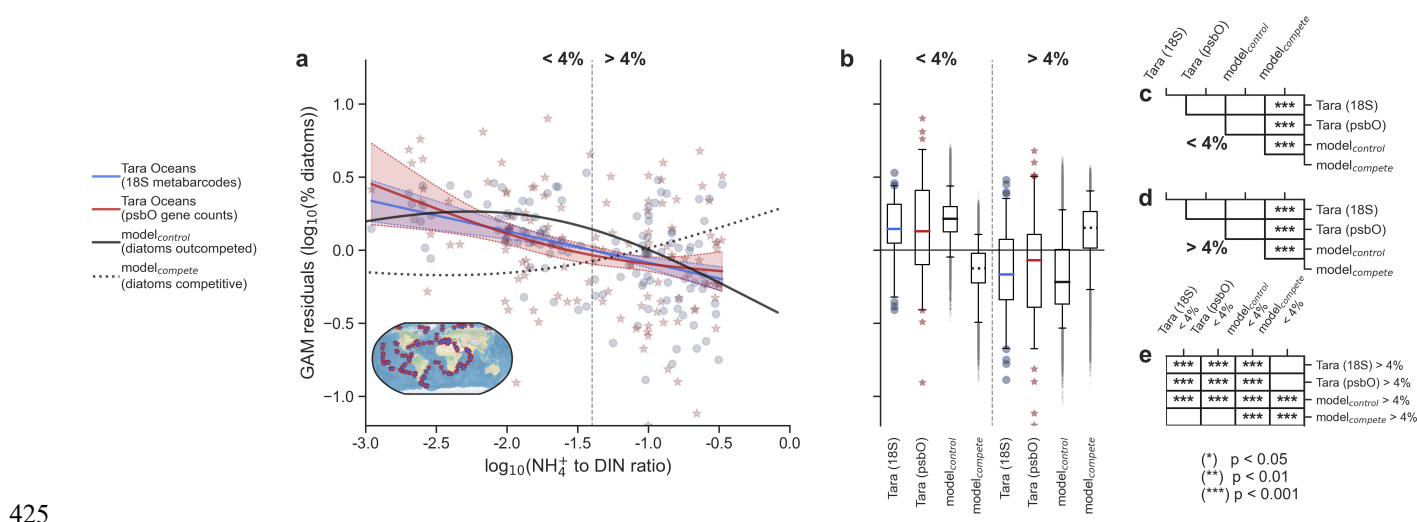
Fig. 5. Effects of NH_4^+ enrichment on primary production and diatom relative abundance. (a), Partial dependence plot from the generalized additive model (GAM) showing the relationship between the NH_4^+ to DIN ratio and the percent relative abundance of diatoms. Blue round markers and blue line fit are percent among eukaryotic phytoplankton (18S rRNA metabarcodes). Red star markers and red line fit are percent among all phytoplankton (*psbO* gene counts). Solid and dashed black lines are output from the ocean-biogeochemical model with
430 and without competitive exclusion of diatoms for NH_4^+. The vertical dotted line delineates when NH_4^+ is 4% of DIN. The inset map shows the locations of *Tara* Oceans samples. (b), Boxplots of the raw partial residuals from panel (a) but separated either side of the 4% NH_4^+ to DIN threshold for percent among eukaryotic phytoplankton (blue), all phytoplankton (red), the ocean-biogeochemical model (solid black), and model without competitive exclusion of diatoms for NH_4^+ (dashed black). Whiskers correspond to the 5th and 95th percentiles. Tables on the right denote significant pair-wise differences (Mann-Whitney U) amongst datasets when NH_4^+:DIN is less than 4% (c), when it is more
435 than 4% (d) and when comparing < 4% with > 4% datasets (e).

3.3.3 Building confidence in the model

To test whether the correct functional relationships emerge from our model, we performed the same GAM analysis that we performed in the previous section on diatom relative abundances predicted by our biogeochemical model. This model lacks a
440 *Prochlorococcus* functional type and so does not allow us to comment on the relative abundance of this type, but does ascribe its diatom functional type with a known competitive disadvantage for NH_4^+ relative to the nanophytoplankton functional type (Fig. 3c). This means that at high NH_4^+:DIN ratios (low NO_3^-) the nanophytoplankton type will always outcompete the diatom type.

445   As expected, the simulated diatom relative abundance was negatively related to NH_4^+:DIN ratios (black line in Fig. 5a; deviance explained = 70%; p-value < 0.001). Interestingly, the relationship was also strongly non-linear and not dissimilar to that seen in the *Tara* Oceans data, with rapid losses of diatoms as NH_4^+:DIN became greater than 4%. This threshold, where NH_4^+ becomes 4% of total nitrogen stocks, aligned with the point at which primary production becomes dominated by regenerated production (Fig. 4). This showcases (1) the intense recycling of NH_4^+ in the marine environment and competition

450   for this coveted nutrient, (2) how diatoms are outcompeted as more primary production becomes regenerated, and (3) how diatoms are major contributors to new primary production in the ocean (Fawcett et al., 2011). Additional statistical analysis showed that on either side of this 4% threshold the GAM predictions built from both the biogeochemical model and *Tara* Oceans data could not be statistically differentiated (Fig. 5b,c,d; Mann-Whitney U pair-wise tests). Both modelled and *Tara* Oceans data predicted similar values of diatom relative abundance within communities where NH_4^+:DIN was less than 4%, as

455   well as in communities where NH_4^+:DIN was greater than 4% (Fig. 5b,e). Overall, the modelled and observed changes in diatom relative abundance associated with NH_4^+:DIN appeared to be similar, at least statistically so. We stress that differences between the biogeochemical model and the *Tara* Oceans data no doubt exist. Nonetheless, the similarity between the model and the observations may mean that the negative relationship between NH_4^+:DIN and diatom relative abundance may indeed originate from the same mechanism, specifically being a competitive disadvantage of diatoms for NH_4^+.

460

3.3.4 The confounding effect of NO_3^-

We fully acknowledge that NH_4^+:DIN ratios covary strongly with NO_3^- concentrations. Most of the projected increases in NH_4^+:DIN we report here are due to circulation changes that limit NO_3^- injection from subsurface waters into surface waters. Also, our GAM analysis of the *Tara* Oceans data could easily be replicated by replacing the NH_4^+:DIN ratio with NO_3^-

465   concentration as a key predictor. Indeed, this analysis showed similar results, with NO_3^- being an equally strong predictor of diatom relative abundance as NH_4^+:DIN. We therefore cannot discount a direct effect of NO_3^- on diatom relative abundance in the *Tara* Oceans observations.

In our biogeochemical model, however, we are able to diagnose whether diatom relative abundance changes are directly due

470   to competition for NO_3^- or NH_4^+. This allows us to assess which of NO_3^- concentration or the NH_4^+:DIN ratio are more appropriate as a predictor. The importance of NH_4^+ is exemplified by the fact that the negative relationship between NH_4^+:DIN and diatom relative abundance was reversed in model$_{compete}$ (black dotted line in Fig. 5a). Now positive rather than negative, this relationship differs statistically from that predicted from *Tara* Oceans data (Figure 5b-e). We therefore suggest that competition for NH_4^+ directly controls diatom relative abundance. While we acknowledge that decreases in NO_3^- were a major

475   cause of NH_4^+ enrichment in our experiments, we emphasize here that a potentially important mechanism of diatom decline in the community is due to their poor competitive ability for growth on NH_4^+, not strictly because of increases or decreases in

total DIN concentration. Decreases in NO_3^- certainly affect diatom growth, but we propose that they mostly do so indirectly by shifting the regime towards intense competition for NH_4^+. Given the statistical similarity between the *in situ* (*Tara* Oceans) and *in silico* (model$_{control}$) relationships, this implicates NH_4^+:DIN as a key underlying driver of diatom relative abundance in

480   the world ocean.

4 Conclusions

Here we have identified a potential enrichment of NH_4^+ in over 98% of ocean euphotic zones by the end of the 21st century under a high emissions scenario (Riahi et al., 2011). We expect that, given the evidence at hand, a widespread increase in NH_4^+-fuelled primary production and shifts in community composition, specifically some negative effects on the competitive

485   niche of diatoms and any other taxa that could be considered NO_3^- specialists and/or poor competitors for NH_4^+. These projections do not differ much from previous work (Bopp et al., 2005), but we recast the attribution of change in terms of competitive exclusion for NH_4^+, rather than bulk nutrient declines. In those places where nitrogen availability limits growth, diatoms suffer displacement by phytoplankton taxa with a greater affinity (i.e., competitive edge) for NH_4^+. The warming and physical changes that we simulate herein, and which drive NH_4^+ enrichment and diatom displacement, are expected (Bindoff

490   et al., 2019), although the high-emissions scenario is now considered less likely than more moderate climate change scenarios. That said, we draw the link between the severity of climate change and the degree of NH_4^+ enrichment, such that our results can be downscaled to consider more moderate scenarios. Also, the link between NH_4^+ enrichment and diatom displacement by more competitive phytoplankton has been demonstrated in numerous previous, albeit localized, studies, and here we demonstrate that it appears also on the global scale using the *Tara* Oceans dataset.

495

Fully ellaboratiung the link between environmental change and NH_4^+ enrichment also rests on many processes that are still not fully understood. For instance, an observed increase in summertime mixed layer depths may counter the effect of a strengthening pycnocline (Sallée et al., 2021) to increase NO_3^- injection into euphotic zones as the ocean continues to respond to climate change. Another good example is the incomplete understanding of the microbial loop and how it responds to

500   environmental change. The microbial loop is driven by heterotrophic bacteria, which resupply NH_4^+ through mineralization of organic matter (Fig. 1). Increases in microbial metabolism were an important driver of the community shifts we projected. Yet, the representation in our model is simplistic. In fact, the microbial loop is not yet incorporated in detail within earth system models in general, but its response to warming can either elevate or depress regenerated production depending on assumptions made about bacterial physiology and function (Cherabier and Ferrière, 2022). The future balance of reduced (NH_4^+ and organic

505   forms) to oxidized nitrogen and its impact on the state of marine ecosystems hinges on a suite of unexplored feedbacks between the marine microbial loop and environmental change. There is much work and research to be done in this space.

Many studies have identified that the open ocean habitat may be becoming more challenging for diatoms and more favourable for small eukaryotes and cyanobacteria. Reductions in NO_3^- supply to the sunlit surface ocean have long been known as an
510 important factor in the predicted loss of diatoms (Bopp et al., 2005). Meanwhile, iron stress appears to be growing in the diatom-dominated Southern Ocean (Ryan-Keogh et al., 2023) and fluctuates strong across climatic modes of variability (Browning et al., 2023), silicic acid limitation is expected across the ocean in response to ocean acidification (Taucher et al., 2022), and growing nitrogen limitation may make diatoms less adaptable as temperatures rise (Aranguren-Gassis et al., 2019). In this study, we add to these potential stressors of diatoms by highlighting the form of DIN. As before, NO_3^- losses are
515 important, but we emphasize that greater competition for NH_4^+ as a consequence of circulation changes and increased recycling, as well as the potential for a more nitrogen-limited Arctic, may further disadvantage diatoms and is expected to give cyanobacteria and other taxa with higher affinities for NH_4^+ a competitive edge. Furthermore, diatoms may be more susceptible to increases in competition for NH_4^+ in temperate waters, as cooler conditions appear to amplify their growth dependence on NO_3^- (Glibert et al., 2016b; Parker and Armbrust, 2005), which is a mechanism that was not incorporated into the model used
520 in this study. Notwithstanding the potential for evolution, these and other rapid changes may reduce diatom diversity (Lampe et al., 2018; Sugie et al., 2020), making diatoms susceptible to extirpation (Cael et al., 2021). If this is realized, ocean ecosystems look to shift towards longer, less productive food-chains underpinned by smaller, slower-growing phytoplankton (Sommer et al., 2002), with severe implications for the health of important fisheries and carbon storage. Further work is urgently needed to understand how the marine nitrogen cycle and key marine phytoplankton groups might respond to these
525 growing challenges in an integrated manner.

Code availability

The model output and scripts to reproduce the analysis are available at https://doi.org/10.5281/zenodo.7630283. Developments to the PISCESv2 ocean-biogeochemical model code are freely available for download at https://github.com/pearseb/ORCA2_OFF_PISCESiso-N.

530 **Data availability**

All data and materials used in the analysis are freely available. Nutrient data, nitrification rates, coincident nutrient concentrations with regenerated/new primary production rates, and ammonia oxidation rates relative to pH variations are provided in Supplementary Data 1-4. The biological data from the *Tara* Oceans sampling program are available at https://zenodo.org/record/3768510#.Xraby6gzY2w and https://ftp.ebi.ac.uk/biostudies/fire/S-BSST/761/S-BSST761/.
535

Author contribution

PJB conceptualized the study, curated the data, lead the analysis, investigation, software (code) development, ran model experiments, visualised the data and wrote the manuscript. JJPK and RET provided data and performed analysis, interpreted the results and contributed writing. RS provided data and visualisation, interpreted the results and edited the manuscript.
540   EMSW provided data, interpretation and edited the manuscript. CB and AT provided funding, computational resources, supervision, interpretation of the results and contributed to the writing and editing of the manuscript.

Competing interest

The authors declare that they have no conflict of interest.

Acknowledgements

545   Simulations and development were undertaken on Barkla, part of the High-Performance Computing facilities at the University of Liverpool. The authors wish to acknowledge use of the Ferret program (http://ferret.pmel.noaa.gov/Ferret/), climate data operators (https://code.mpimet.mpg.de/projects/cdo/), NetCDF Operators (http://nco.sourceforge.net/) and Python (www.python.org) for the analysis and graphics in this paper. Thanks to Xianhui Wan, Carolyn Buchwald and Alyson Santoro who shared data, and ongoing discussions with Elena Litchman and Tyler Rohr.

550   **Financial support**

PJB, RET and AT were supported by the ARISE project (NE/P006035/1), part of the Changing Arctic Ocean programme, jointly funded by the UKRI Natural Environmental Research Council (NERC) and the German Federal Ministry of Education and Research (BMBF). JJPK was supported by the Moore-Simons Project on the Origin of the Eukaryotic Cell, Simons Foundation (735929LPI). EMSW and AT acknowledge support from the UKRI NERC grant NE/N009525/1, the Mid Atlantic
555   Ridge project (FRidge). EMSW was also supported by the UKRI NERC grant NE/N001079/1 (Zinc, Iron and Phosphorus in the Atlantic). RET also acknowledges support from the UKRI NERC grant NE/W009536/1. CB acknowledges support from FEM (Fonds Francais pour l'Environnement Mondial), the French Government 'Investissements d'Avenir' programs OCEANOMICS (ANR-11-BTBR-0008), FRANCE GENOMIQUE (ANR-10-INBS-09-08), MEMO LIFE (ANR-10-LABX-54), and PSL Research University (ANR-11-IDEX-0001-02), the European Research Council (ERC) under the European
560   Union's Horizon 2020 research and innovation program (Diatomic; grant agreement No. 835067), and project AtlantECO.

References

Andersen, I. M., Williamson, T. J., González, M. J., and Vanni, M. J.: Nitrate, ammonium, and phosphorus drive seasonal nutrient limitation of chlorophytes, cyanobacteria, and diatoms in a hyper-eutrophic reservoir, Limnol Oceanogr, 65, 962–978, https://doi.org/10.1002/lno.11363, 2020.

565   Anderson, S. I., Barton, A. D., Clayton, S., Dutkiewicz, S., and Rynearson, T. A.: Marine phytoplankton functional types exhibit diverse responses to thermal change, Nat Commun, 12, 6413, https://doi.org/10.1038/s41467-021-26651-8, 2021.

Aranguren-Gassis, M., Kremer, C. T., Klausmeier, C. A., and Litchman, E.: Nitrogen limitation inhibits marine diatom adaptation to high temperatures, Ecol Lett, 22, 1860–1869, https://doi.org/10.1111/ele.13378, 2019.

Aumont, O., Ethé, C., Tagliabue, A., Bopp, L., and Gehlen, M.: PISCES-v2: an ocean biogeochemical model for carbon and

570   ecosystem studies, Geosci Model Dev, 8, 2465–2513, https://doi.org/10.5194/gmd-8-2465-2015, 2015.

Bayer, B., Vojvoda, J., Offre, P., Alves, R. J. E., Elisabeth, N. H., Garcia, J. AL, Volland, J.-M., Srivastava, A., Schleper, C., and Herndl, G. J.: Physiological and genomic characterization of two novel marine thaumarchaeal strains indicates niche differentiation, ISME J, 10, 1051–1063, https://doi.org/10.1038/ismej.2015.200, 2016.

Beman, J. M., Chow, C. E., King, A. L., Feng, Y., Fuhrman, J. A., Andersson, A., Bates, N. R., Popp, B. N., and Hutchins, D.

575   A.: Global declines in oceanic nitrification rates as a consequence of ocean acidification, Proc Natl Acad Sci U S A, 108, 208–213, https://doi.org/10.1073/pnas.1011053108, 2011.

Bender, M. L. and Jönsson, B.: Is seasonal net community production in the South Pacific Subtropical Gyre anomalously low?, Geophys Res Lett, 43, 9757–9763, https://doi.org/10.1002/2016GL070220, 2016.

Berg, G., Balode, M., Purina, I., Bekere, S., Béchemin, C., and Maestrini, S.: Plankton community composition in relation to

580   availability and uptake of oxidized and reduced nitrogen, Aquatic Microbial Ecology, 30, 263–274, https://doi.org/10.3354/ame030263, 2003.

Bindoff, N. L., Cheung, W. W. L., Kairo, J. G., Aristegui, J., Guinder, V. A., Hallberg, R., Hilmi, N., Jiao, N., Karim, M. S., Levin, L., O'Donoghue, S., Purca Cuicapusa, S. R., Rinkevich, B., Suga, T., Tagliabue, A., and Williamson, P.: Changing Ocean, Marine Ecosystems, and Dependent Communities, in: IPCC Special Report on the Ocean and Cryosphere in a Changing

585   Climate, edited by: Portner, H.-O., Roberts, C. D., Masson-Delmotte, V., Zhai, P., Tignor, E., Poloczanska, E., Mintenbeck, K., Alegria, A., Nicolai, M., Okem, A., Petzold, J., Rama, B., and Weyer, N. M., 447–588, https://doi.org/https://www.ipcc.ch/report/srocc/, 2019.

Bopp, L., Aumont, O., Cadule, P., Alvain, S., and Gehlen, M.: Response of diatoms distribution to global warming and potential implications: A global model study, Geophys Res Lett, 32, n/a-n/a, https://doi.org/10.1029/2005GL023653, 2005.

590   Boyd, P. W., LaRoche, J., Gall, M., Frew, R., and McKay, R. M. L.: Role of iron, light, and silicate in controlling algal biomass in subantarctic waters SE of New Zealand, J Geophys Res Oceans, 104, 13395–13408, https://doi.org/10.1029/1999JC900009, 1999.

Boyd, P. W., Watson, A. J., Law, C. S., Abraham, E. R., Trull, T., Murdoch, R., Bakker, D. C. E., Bowie, A. R., Buesseler, K. O., Chang, H., Charette, M., Croot, P., Downing, K., Frew, R., Gall, M., Hadfield, M., Hall, J., Harvey, M., Jameson, G.,
595 LaRoche, J., Liddicoat, M., Ling, R., Maldonado, M. T., McKay, R. M., Nodder, S., Pickmere, S., Pridmore, R., Rintoul, S., Safi, K., Sutton, P., Strzepek, R., Tanneberger, K., Turner, S., Waite, A., and Zeldis, J.: A mesoscale phytoplankton bloom in the polar Southern Ocean stimulated by iron fertilization, Nature, 407, 695–702, https://doi.org/10.1038/35037500, 2000.

Browning, T. J., Saito, M. A., Garaba, S. P., Wang, X., Achterberg, E. P., Moore, C. M., Engel, A., McIlvin, M. R., Moran, D., Voss, D., Zielinski, O., and Tagliabue, A.: Persistent equatorial Pacific iron limitation under ENSO forcing, Nature,
600 https://doi.org/10.1038/s41586-023-06439-0, 2023.

Brun, P., Vogt, M., Payne, M. R., Gruber, N., O'Brien, C. J., Buitenhuis, E. T., Le Quéré, C., Leblanc, K., and Luo, Y.-W.: Ecological niches of open ocean phytoplankton taxa, Limnol Oceanogr, 60, 1020–1038, https://doi.org/10.1002/lno.10074, 2015.

Buchanan, P. J., Aumont, O., Bopp, L., Mahaffey, C., and Tagliabue, A.: Impact of intensifying nitrogen limitation on ocean
605 net primary production is fingerprinted by nitrogen isotopes, Nat Commun, 12, 6214, https://doi.org/10.1038/s41467-021-26552-w, 2021.

Buchwald, C., Santoro, A. E., Stanley, R. H. R., and Casciotti, K. L.: Nitrogen cycling in the secondary nitrite maximum of the eastern tropical North Pacific off Costa Rica, Global Biogeochem Cycles, 29, 2061–2081, https://doi.org/10.1002/2015GB005187, 2015.

610 Cael, B. B., Dutkiewicz, S., and Henson, S.: Abrupt shifts in 21st-century plankton communities, Sci Adv, 7, https://doi.org/10.1126/sciadv.abf8593, 2021.

Carter, C. M., Ross, A. H., Schiel, D. R., Howard-Williams, C., and Hayden, B.: In situ microcosm experiments on the influence of nitrate and light on phytoplankton community composition, J Exp Mar Biol Ecol, 326, 1–13, https://doi.org/10.1016/j.jembe.2005.05.006, 2005.

615 Chen, B., Landry, M. R., Huang, B., and Liu, H.: Does warming enhance the effect of microzooplankton grazing on marine phytoplankton in the ocean?, Limnol Oceanogr, 57, 519–526, https://doi.org/10.4319/lo.2012.57.2.0519, 2012.

Cherabier, P. and Ferrière, R.: Eco-evolutionary responses of the microbial loop to surface ocean warming and consequences for primary production, ISME Journal, 16, 1130–1139, https://doi.org/10.1038/s41396-021-01166-8, 2022.

Clark, D. R., Rees, A. P., and Joint, I.: Ammonium regeneration and nitrification rates in the oligotrophic Atlantic Ocean:
620 Implications for new production estimates, Limnol Oceanogr, 53, 52–62, https://doi.org/10.4319/lo.2008.53.1.0052, 2008.

Clark, D. R., Rees, A. P., Ferrera, C., Al-moosawi, L., Somerfield, P. J., Harris, C., Quartly, G. D., Goult, S., Tarran, G., and Lessin, G.: Nitrification in the oligotrophic Atlantic Ocean, Biogeosciences Discussions, 1–29, https://doi.org/10.5194/bg-2021-184, 2021.

Comeau, A. M., Li, W. K. W., Tremblay, J.-É., Carmack, E. C., and Lovejoy, C.: Arctic Ocean Microbial Community Structure
625 before and after the 2007 Record Sea Ice Minimum, PLoS One, 6, e27492, https://doi.org/10.1371/journal.pone.0027492, 2011.

Donald, D. B., Bogard, M. J., Finlay, K., Bunting, L., and Leavitt, P. R.: Phytoplankton-Specific Response to Enrichment of Phosphorus-Rich Surface Waters with Ammonium, Nitrate, and Urea, PLoS One, 8, e53277, https://doi.org/10.1371/journal.pone.0053277, 2013.

630 Dore, J. E. and Karl, D. M.: Nitrification in the euphotic zone as a source for nitrite, nitrate, and nitrous oxide at Station ALOHA, Limnol Oceanogr, 41, 1619–1628, https://doi.org/10.4319/lo.1996.41.8.1619, 1996.

Dortch, Q.: The interaction between ammonium and nitrate uptake in phytoplankton, Mar Ecol Prog Ser, 61, 183–201, https://doi.org/10.3354/meps061183, 1990.

Dufresne, J. L., Foujols, M. A., Denvil, S., Caubel, A., Marti, O., Aumont, O., Balkanski, Y., Bekki, S., Bellenger, H., Benshila,
635 R., Bony, S., Bopp, L., Braconnot, P., Brockmann, P., Cadule, P., Cheruy, F., Codron, F., Cozic, A., Cugnet, D., de Noblet, N., Duvel, J. P., Ethé, C., Fairhead, L., Fichefet, T., Flavoni, S., Friedlingstein, P., Grandpeix, J. Y., Guez, L., Guilyardi, E., Hauglustaine, D., Hourdin, F., Idelkadi, A., Ghattas, J., Joussaume, S., Kageyama, M., Krinner, G., Labetoulle, S., Lahellec, A., Lefebvre, M. P., Lefevre, F., Levy, C., Li, Z. X., Lloyd, J., Lott, F., Madec, G., Mancip, M., Marchand, M., Masson, S., Meurdesoif, Y., Mignot, J., Musat, I., Parouty, S., Polcher, J., Rio, C., Schulz, M., Swingedouw, D., Szopa, S., Talandier, C.,
640 Terray, P., Viovy, N., and Vuichard, N.: Climate change projections using the IPSL-CM5 Earth System Model: From CMIP3 to CMIP5, 2123–2165 pp., https://doi.org/10.1007/s00382-012-1636-1, 2013.

Dugdale, R. C.: Nutrient limitation in the Sea: Dynamics, identification, and significance, Limnol Oceanogr, 12, 685–695, 1967.

Dugdale, R. C. and Goering, J. J.: Uptake of New and Regenerated Forms of Nitrogen in Primary Productivity, Limnol
645 Oceanogr, 12, 196–206, https://doi.org/10.4319/lo.1967.12.2.0196, 1967.

Eppley, R. W.: Temperature and phytoplankton growth in the sea, Fishery Bulletin, 70, 1063–1085, 1972.

Fawcett, S. E., Lomas, M. W., Casey, J. R., Ward, B. B., and Sigman, D. M.: Assimilation of upwelled nitrate by small eukaryotes in the Sargasso Sea, Nat Geosci, 4, 717–722, https://doi.org/10.1038/ngeo1265, 2011.

Fernández, C., Farías, L., and Alcaman, M. E.: Primary production and nitrogen regeneration processes in surface waters of
650 the Peruvian upwelling system, Prog Oceanogr, 83, 159–168, https://doi.org/10.1016/j.pocean.2009.07.010, 2009.

Follows, M. J., Dutkiewicz, S., Grant, S., and Chisholm, S. W.: Emergent Biogeography of Microbial Communities in a Model Ocean, Science (1979), 315, 1843–1846, https://doi.org/10.1126/science.1138544, 2007.

Garcia, H. E., Weathers, K. W., Paver, C. R., Smolyar, I., Boyer, T. P., Locarnini, R. A., Zweng, M. M., Mishonov, A. V., Baranova, O. K., Seidov, D., and Reagan, J. R.: World Ocean Atlas 2018. Volume 4: Dissolved Inorganic Nutrients
655 (phosphate, nitrate and nitrate+nitrite, silicate)., edited by: Editor, A. M. T., 35 pp., 2019.

Glibert, P. M., Wilkerson, F. P., Dugdale, R. C., Raven, J. A., Dupont, C. L., Leavitt, P. R., Parker, A. E., Burkholder, J. M., and Kana, T. M.: Pluses and minuses of ammonium and nitrate uptake and assimilation by phytoplankton and implications for productivity and community composition, with emphasis on nitrogen-enriched conditions, Limnol Oceanogr, 61, 165–197, https://doi.org/10.1002/lno.10203, 2016a.

660   Glibert, P. M., Wilkerson, F. P., Dugdale, R. C., Raven, J. A., Dupont, C. L., Leavitt, P. R., Parker, A. E., Burkholder, J. M., and Kana, T. M.: Pluses and minuses of ammonium and nitrate uptake and assimilation by phytoplankton and implications for productivity and community composition, with emphasis on nitrogen-enriched conditions, Limnol Oceanogr, 61, 165–197, https://doi.org/10.1002/lno.10203, 2016b.

Herrero, A., Muro-Pastor, A. M., and Flores, E.: Nitrogen Control in Cyanobacteria, J Bacteriol, 183, 411–425,
665   https://doi.org/10.1128/JB.183.2.411-425.2001, 2001.

Huesemann, M. H., Skillman, A. D., and Crecelius, E. A.: The inhibition of marine nitrification by ocean disposal of carbon dioxide, Mar Pollut Bull, 44, 142–148, https://doi.org/10.1016/S0025-326X(01)00194-1, 2002.

Ibarbalz, F. M., Henry, N., Brandão, M. C., Martini, S., Busseni, G., Byrne, H., Coelho, L. P., Endo, H., Gasol, J. M., Gregory, A. C., Mahé, F., Rigonato, J., Royo-Llonch, M., Salazar, G., Sanz-Sáez, I., Scalco, E., Soviadan, D., Zayed, A. A., Zingone,
670   A., Labadie, K., Ferland, J., Marec, C., Kandels, S., Picheral, M., Dimier, C., Poulain, J., Pisarev, S., Carmichael, M., Pesant, S., Babin, M., Boss, E., Iudicone, D., Jaillon, O., Acinas, S. G., Ogata, H., Pelletier, E., Stemmann, L., Sullivan, M. B., Sunagawa, S., Bopp, L., de Vargas, C., Karp-Boss, L., Wincker, P., Lombard, F., Bowler, C., Zinger, L., Acinas, S. G., Babin, M., Bork, P., Boss, E., Bowler, C., Cochrane, G., de Vargas, C., Follows, M., Gorsky, G., Grimsley, N., Guidi, L., Hingamp, P., Iudicone, D., Jaillon, O., Kandels, S., Karp-Boss, L., Karsenti, E., Not, F., Ogata, H., Pesant, S., Poulton, N., Raes, J.,
675   Sardet, C., Speich, S., Stemmann, L., Sullivan, M. B., Sunagawa, S., and Wincker, P.: Global Trends in Marine Plankton Diversity across Kingdoms of Life, Cell, 179, 1084-1097.e21, https://doi.org/10.1016/j.cell.2019.10.008, 2019.

Joubert, W. R., Thomalla, S. J., Waldron, H. N., Lucas, M. I., Boye, M., Le Moigne, F. A. C., Planchon, F., and Speich, S.: Nitrogen uptake by phytoplankton in the Atlantic sector of the Southern Ocean during late austral summer, Biogeosciences, 8, 2947–2959, https://doi.org/10.5194/bg-8-2947-2011, 2011.

680   Kitidis, V., Laverock, B., McNeill, L. C., Beesley, A., Cummings, D., Tait, K., Osborn, M. A., and Widdicombe, S.: Impact of ocean acidification on benthic and water column ammonia oxidation, Geophys Res Lett, 38, n/a-n/a, https://doi.org/10.1029/2011GL049095, 2011.

Klawonn, I., Bonaglia, S., Whitehouse, M. J., Littmann, S., Tienken, D., Kuypers, M. M. M., Brüchert, V., and Ploug, H.: Untangling hidden nutrient dynamics: rapid ammonium cycling and single-cell ammonium assimilation in marine plankton
685   communities, ISME J, 13, 1960–1974, https://doi.org/10.1038/s41396-019-0386-z, 2019.

Krumhardt, K. M., Long, M. C., Sylvester, Z. T., and Petrik, C. M.: Climate drivers of Southern Ocean phytoplankton community composition and potential impacts on higher trophic levels, Front Mar Sci, 9, https://doi.org/10.3389/fmars.2022.916140, 2022.

Kwiatkowski, L., Torres, O., Bopp, L., Aumont, O., Chamberlain, M., Christian, J. R., Dunne, J. P., Gehlen, M., Ilyina, T.,
690   John, J. G., Lenton, A., Li, H., Lovenduski, N. S., Orr, J. C., Palmieri, J., Santana-Falcón, Y., Schwinger, J., Séférian, R., Stock, C. A., Tagliabue, A., Takano, Y., Tjiputra, J., Toyama, K., Tsujino, H., Watanabe, M., Yamamoto, A., Yool, A., and Ziehn, T.: Twenty-first century ocean warming, acidification, deoxygenation, and upper-ocean nutrient and primary production decline from CMIP6 model projections, Biogeosciences, 17, 3439–3470, https://doi.org/10.5194/bg-17-3439-2020, 2020.

Lampe, R. H., Mann, E. L., Cohen, N. R., Till, C. P., Thamatrakoln, K., Brzezinski, M. A., Bruland, K. W., Twining, B. S.,
695 and Marchetti, A.: Different iron storage strategies among bloom-forming diatoms, Proceedings of the National Academy of
Sciences, 115, E12275–E12284, https://doi.org/10.1073/pnas.1805243115, 2018.

Litchman, E.: Resource Competition and the Ecological Success of Phytoplankton, in: Evolution of Primary Producers in the
Sea, Elsevier, 351–375, https://doi.org/10.1016/B978-012370518-1/50017-5, 2007.

Litchman, E., Klausmeier, C. A., Schofield, O. M., and Falkowski, P. G.: The role of functional traits and trade-offs in
700 structuring phytoplankton communities: scaling from cellular to ecosystem level, Ecol Lett, 10, 1170–1181,
https://doi.org/10.1111/j.1461-0248.2007.01117.x, 2007.

Llort, J., Lévy, M., Sallée, J. B., and Tagliabue, A.: Nonmonotonic Response of Primary Production and Export to Changes in
Mixed-Layer Depth in the Southern Ocean, Geophys Res Lett, 2018GL081788, https://doi.org/10.1029/2018GL081788, 2019.

Lomas, M. W. and Glibert, P. M.: Temperature regulation of nitrate uptake: A novel hypothesis about nitrate uptake and
705 reduction in cool-water diatoms, Limnol Oceanogr, 44, 556–572, https://doi.org/10.4319/lo.1999.44.3.0556, 1999.

Margalef, R.: Life-forms of phytoplankton as survival alternatives in an unstable environment, Oceanologica Acta, 1, 493–
509, 1978.

Matsumoto, K., Abe, O., Fujiki, T., Sukigara, C., and Mino, Y.: Primary productivity at the time-series stations in the
northwestern Pacific Ocean: is the subtropical station unproductive?, J Oceanogr, 72, 359–371,
710 https://doi.org/10.1007/s10872-016-0354-4, 2016.

Mdutyana, M., Thomalla, S. J., Philibert, R., Ward, B. B., and Fawcett, S. E.: The Seasonal Cycle of Nitrogen Uptake and
Nitrification in the Atlantic Sector of the Southern Ocean, Global Biogeochem Cycles, 34, 1–29,
https://doi.org/10.1029/2019GB006363, 2020.

Metzler, P. M., Glibert, P. M., Gaeta, S. A., and Ludlam, J. M.: New and regenerated production in the South Atlantic off
715 Brazil, Deep Sea Research Part I: Oceanographic Research Papers, 44, 363–384, https://doi.org/10.1016/S0967-
0637(96)00129-X, 1997.

Newell, S. E., Fawcett, S. E., and Ward, B. B.: Depth distribution of ammonia oxidation rates and ammonia-oxidizer
community composition in the Sargasso Sea, Limnol Oceanogr, 58, 1491–1500, https://doi.org/10.4319/lo.2013.58.4.1491,
2013.

720 Van Oostende, N., Fawcett, S. E., Marconi, D., Lueders-Dumont, J., Sabadel, A. J. M., Woodward, E. M. S., Jönsson, B. F.,
Sigman, D. M., and Ward, B. B.: Variation of summer phytoplankton community composition and its relationship to nitrate
and regenerated nitrogen assimilation across the North Atlantic Ocean, Deep Sea Research Part I: Oceanographic Research
Papers, 121, 79–94, https://doi.org/10.1016/j.dsr.2016.12.012, 2017.

Örnólfsdóttir, E. B., Lumsden, S. E., and Pinckney, J. L.: Nutrient pulsing as a regulator of phytoplankton abundance and
725 community composition in Galveston Bay, Texas, J Exp Mar Biol Ecol, 303, 197–220,
https://doi.org/10.1016/j.jembe.2003.11.016, 2004.

Parker, M. S. and Armbrust, E. V.: Synergistic effects of light, temperature, and nitrogen source on transcription of genes for carbon and nitrogen metabolism in the centric diatom Thalassiosira Pseudonana (Bacillariophycae), J Phycol, 41, 1142–1153, https://doi.org/10.1111/j.1529-8817.2005.00139.x, 2005.

730   Philibert, M. C. R.: A comparative study of nitrogen uptake and nitrification rates in sub-tropical, polar and upwelling waters, University of Cape Town, 2015.

Pierella Karlusich, J. J., Ibarbalz, F. M., and Bowler, C.: Phytoplankton in the *Tara* Ocean, Ann Rev Mar Sci, 12, 233–265, https://doi.org/10.1146/annurev-marine-010419-010706, 2020.

Pierella Karlusich, J. J., Pelletier, E., Zinger, L., Lombard, F., Zingone, A., Colin, S., Gasol, J. M., Dorrell, R. G., Henry, N.,

735   Scalco, E., Acinas, S. G., Wincker, P., de Vargas, C., and Bowler, C.: A robust approach to estimate relative phytoplankton cell abundances from metagenomes, Mol Ecol Resour, 23, 16–40, https://doi.org/10.1111/1755-0998.13592, 2023.

Raes, E. J., van de Kamp, J., Bodrossy, L., Fong, A. A., Riekenberg, J., Holmes, B. H., Erler, D. V., Eyre, B. D., Weil, S.-S., and Waite, A. M.: N2 Fixation and New Insights Into Nitrification From the Ice-Edge to the Equator in the South Pacific Ocean, Front Mar Sci, 7, 1–20, https://doi.org/10.3389/fmars.2020.00389, 2020.

740   Raimbault, P., Slawyk, G., Boudjellal, B., Coatanoan, C., Conan, P., Coste, B., Garcia, N., Moutin, T., and Pujo-Pay, M.: Carbon and nitrogen uptake and export in the equatorial Pacific at 150°W: Evidence of an efficient regenerated production cycle, J Geophys Res Oceans, 104, 3341–3356, https://doi.org/10.1029/1998JC900004, 1999.

Rees, A. P., Woodward, E. M. S., and Joint, I.: Concentrations and uptake of nitrate and ammonium in the Atlantic Ocean between 60°N and 50°S, Deep Sea Research Part II: Topical Studies in Oceanography, 53, 1649–1665,

745   https://doi.org/10.1016/j.dsr2.2006.05.008, 2006.

Riahi, K., Rao, S., Krey, V., Cho, C., Chirkov, V., Fischer, G., Kindermann, G., Nakicenovic, N., and Rafaj, P.: RCP 8.5—A scenario of comparatively high greenhouse gas emissions, Clim Change, 109, 33–57, https://doi.org/10.1007/s10584-011-0149-y, 2011.

Riahi, K., van Vuuren, D. P., Kriegler, E., Edmonds, J., O'Neill, B. C., Fujimori, S., Bauer, N., Calvin, K., Dellink, R., Fricko,

750   O., Lutz, W., Popp, A., Cuaresma, J. C., KC, S., Leimbach, M., Jiang, L., Kram, T., Rao, S., Emmerling, J., Ebi, K., Hasegawa, T., Havlik, P., Humpenöder, F., Da Silva, L. A., Smith, S., Stehfest, E., Bosetti, V., Eom, J., Gernaat, D., Masui, T., Rogelj, J., Strefler, J., Drouet, L., Krey, V., Luderer, G., Harmsen, M., Takahashi, K., Baumstark, L., Doelman, J. C., Kainuma, M., Klimont, Z., Marangoni, G., Lotze-Campen, H., Obersteiner, M., Tabeau, A., and Tavoni, M.: The Shared Socioeconomic Pathways and their energy, land use, and greenhouse gas emissions implications: An overview, Global Environmental Change,

755   42, 153–168, https://doi.org/10.1016/j.gloenvcha.2016.05.009, 2017.

Rii, Y., Karl, D., and Church, M.: Temporal and vertical variability in picophytoplankton primary productivity in the North Pacific Subtropical Gyre, Mar Ecol Prog Ser, 562, 1–18, https://doi.org/10.3354/meps11954, 2016.

Rodgers, K. B., Aumont, O., Toyama, K., Resplandy, L., Ishii, M., Nakano, T., Sasano, D., Bianchi, D., and Yamaguchi, R.: Low-latitude mesopelagic nutrient recycling controls productivity and export, Nature, 632, 802–807,

760   https://doi.org/10.1038/s41586-024-07779-1, 2024.

Rohr, T., Richardson, A. J., Lenton, A., Chamberlain, M. A., and Shadwick, E. H.: Zooplankton grazing is the largest source of uncertainty for marine carbon cycling in CMIP6 models, Commun Earth Environ, 4, https://doi.org/10.1038/s43247-023-00871-w, 2023.

Ryan-Keogh, T. J., Thomalla, S. J., Monteiro, P. M. S., and Tagliabue, A.: Multidecadal trend of increasing iron stress in

765   Southern Ocean phytoplankton, Science (1979), 379, 834–840, https://doi.org/10.1126/science.abl5237, 2023.

Sallée, J., Pellichero, V., Akhoudas, C., Pauthenet, E., Vignes, L., Schmidtko, S., Garabato, A. N., Sutherland, P., and Kuusela, M.: Summertime increases in upper-ocean stratification and mixed-layer depth, Nature, 591, 592–598, https://doi.org/10.1038/s41586-021-03303-x, 2021.

Santoro, A. E., Sakamoto, C. M., Smith, J. M., Plant, J. N., Gehman, A. L., Worden, A. Z., Johnson, K. S., Francis, C. A., and

770   Casciotti, K. L.: Measurements of nitrite production in and around the primary nitrite maximum in the central California Current, Biogeosciences, 10, 7395–7410, https://doi.org/10.5194/bg-10-7395-2013, 2013.

Santoro, A. E., Buchwald, C., Knapp, A. N., Berelson, W. M., Capone, D. G., and Casciotti, K. L.: Nitrification and Nitrous Oxide Production in the Offshore Waters of the Eastern Tropical South Pacific, Global Biogeochem Cycles, 35, 1–21, https://doi.org/10.1029/2020GB006716, 2021.

775   Selph, K. E., Swalethorp, R., Stukel, M. R., Kelly, T. B., Knapp, A. N., Fleming, K., Hernandez, T., and Landry, M. R.: Phytoplankton community composition and biomass in the oligotrophic Gulf of Mexico, J Plankton Res, 1–20, https://doi.org/10.1093/plankt/fbab006, 2021.

Shiozaki, T., Ijichi, M., Isobe, K., Hashihama, F., Nakamura, K., Ehama, M., Hayashizaki, K., Takahashi, K., Hamasaki, K., and Furuya, K.: Nitrification and its influence on biogeochemical cycles from the equatorial Pacific to the Arctic Ocean, ISME

780   J, 10, 2184–2197, https://doi.org/10.1038/ismej.2016.18, 2016.

Sommer, U., Stibor, H., Katechakis, A., Sommer, F., and Hansen, T.: Pelagic food web configurations at different levels of nutrient richness and their implications for the ratio fish production:primary production, Hydrobiologia, 484, 11–20, https://doi.org/10.1023/A:1021340601986, 2002.

Sugie, K., Fujiwara, A., Nishino, S., Kameyama, S., and Harada, N.: Impacts of Temperature, CO2, and Salinity on

785   Phytoplankton Community Composition in the Western Arctic Ocean, Front Mar Sci, 6, https://doi.org/10.3389/fmars.2019.00821, 2020.

Taucher, J., Bach, L. T., Prowe, A. E. F., Boxhammer, T., Kvale, K., and Riebesell, U.: Enhanced silica export in a future ocean triggers global diatom decline, Nature, 605, 696–700, https://doi.org/10.1038/s41586-022-04687-0, 2022.

Thomalla, S. J., Waldron, H. N., Lucas, M. I., Read, J. F., Ansorge, I. J., and Pakhomov, E.: Phytoplankton distribution and

790   nitrogen dynamics in the southwest indian subtropical gyre and Southern Ocean waters, Ocean Science, 7, 113–127, https://doi.org/10.5194/os-7-113-2011, 2011.

Tolar, B. B., Ross, M. J., Wallsgrove, N. J., Liu, Q., Aluwihare, L. I., Popp, B. N., and Hollibaugh, J. T.: Contribution of ammonia oxidation to chemoautotrophy in Antarctic coastal waters, ISME J, 10, 2605–2619, https://doi.org/10.1038/ismej.2016.61, 2016.

795 Trommer, G., Poxleitner, M., and Stibor, H.: Responses of lake phytoplankton communities to changing inorganic nitrogen supply forms, Aquat Sci, 82, 22, https://doi.org/10.1007/s00027-020-0696-2, 2020.

Tungaraza, C., Rousseau, V., Brion, N., Lancelot, C., Gichuki, J., Baeyens, W., and Goeyens, L.: Contrasting nitrogen uptake by diatom and Phaeocystis-dominated phytoplankton assemblages in the North Sea, J Exp Mar Biol Ecol, 292, 19–41, https://doi.org/10.1016/S0022-0981(03)00145-X, 2003.

800 Vannier, T., Leconte, J., Seeleuthner, Y., Mondy, S., Pelletier, E., Aury, J.-M., de Vargas, C., Sieracki, M., Iudicone, D., Vaulot, D., Wincker, P., and Jaillon, O.: Survey of the green picoalga Bathycoccus genomes in the global ocean, Sci Rep, 6, 37900, https://doi.org/10.1038/srep37900, 2016.

de Vargas, C., Audic, S., Henry, N., Decelle, J., Mahé, F., Logares, R., Lara, E., Berney, C., Le Bescot, N., Probert, I., Carmichael, M., Poulain, J., Romac, S., Colin, S., Aury, J.-M., Bittner, L., Chaffron, S., Dunthorn, M., Engelen, S., Flegontova,

805 O., Guidi, L., Horák, A., Jaillon, O., Lima-Mendez, G., Lukeš, J., Malviya, S., Morard, R., Mulot, M., Scalco, E., Siano, R., Vincent, F., Zingone, A., Dimier, C., Picheral, M., Searson, S., Kandels-Lewis, S., Acinas, S. G., Bork, P., Bowler, C., Gorsky, G., Grimsley, N., Hingamp, P., Iudicone, D., Not, F., Ogata, H., Pesant, S., Raes, J., Sieracki, M. E., Speich, S., Stemmann, L., Sunagawa, S., Weissenbach, J., Wincker, P., Karsenti, E., Boss, E., Follows, M., Karp-Boss, L., Krzic, U., Reynaud, E. G., Sardet, C., Sullivan, M. B., and Velayoudon, D.: Eukaryotic plankton diversity in the sunlit ocean, Science (1979), 348,

810 https://doi.org/10.1126/science.1261605, 2015.

Wan, X. S., Sheng, H.-X., Dai, M., Zhang, Y., Shi, D., Trull, T. W., Zhu, Y., Lomas, M. W., and Kao, S.-J.: Ambient nitrate switches the ammonium consumption pathway in the euphotic ocean, Nat Commun, 9, 915, https://doi.org/10.1038/s41467-018-03363-0, 2018.

Wan, X. S., Sheng, H., Dai, M., Church, M. J., Zou, W., Li, X., Hutchins, D. A., Ward, B. B., and Kao, S.: Phytoplankton-

815 Nitrifier Interactions Control the Geographic Distribution of Nitrite in the Upper Ocean, Global Biogeochem Cycles, 35, 1–19, https://doi.org/10.1029/2021GB007072, 2021.

Whitt, D. B. and Jansen, M. F.: Slower nutrient stream suppresses Subarctic Atlantic Ocean biological productivity in global warming, Proceedings of the National Academy of Sciences, 117, 15504–15510, https://doi.org/10.1073/pnas.2000851117, 2020.

820 Wood, S. N.: Generalized Additive Models, Chapman and Hall/CRC, https://doi.org/10.1201/9781420010404, 2006.

Yang, B., Emerson, S. R., and Quay, P. D.: The Subtropical Ocean's Biological Carbon Pump Determined From O 2 and DIC/DI 13 C Tracers, Geophys Res Lett, 46, 5361–5368, https://doi.org/10.1029/2018GL081239, 2019.

Yingling, N., Kelly, T. B., Shropshire, T. A., Landry, M. R., Selph, K. E., Knapp, A. N., Kranz, S. A., and Stukel, M. R.: Taxon-specific phytoplankton growth, nutrient utilization and light limitation in the oligotrophic Gulf of Mexico, J Plankton

825 Res, 1–21, https://doi.org/10.1093/plankt/fbab028, 2021.

Yool, A., Martin, A. P., Fernández, C., and Clark, D. R.: The significance of nitrification for oceanic new production., Nature, 447, 999–1002, https://doi.org/10.1038/nature05885, 2007.